ELSEVIER

Biophysical Chemistry 105 (2003) 639–648

Biophysical Chemistry

www.elsevier.com/locate/bpc

Hemodextrin: a self-assembled cyclodextrin–porphyrin construct that binds dioxygen

Huchen Zhou, John T. Groves*

Department of Chemistry, Princeton University, Princeton, NJ 08544, USA

Received 14 November 2002; received in revised form 13 February 2003; accepted 13 February 2003

Abstract

Synthetic hemoprotein model compounds are of great interest due to the vital roles and complexities of hemoproteins. This study reports a novel, self-assembled hemoprotein model, hemodextrin. The synthesis and characterization of py-PPCD (2^{A}-monopyridylmethyl-perPEGylated-β-cyclodextrin) (**2**) is described. The molecular design is based on a pegylated cyclodextrin scaffold that bears both a heme-binding pocket and an axial ligand that binds an iron porphyrin. The binding constant for Fe(III)TPPS [iron(III) *meso*-tetra(4-sulphonatophenyl)porphyrin] by py-PPCD (**2**) was determined to be 2×10^{6} M^{-1} at pH 6.0 by observing characteristic changes in the UV–Vis spectrum of the porphyrin. The pyridyl nitrogen of py-PPCD (**2**) was shown to ligate to the iron center by observing signal changes in the Fe(II)-porphyrin ^{1}H-NMR spectrum. This hemodextrin ensemble was shown to bind dioxygen reversibly and to form a stable ferryl species.

Keywords: Cyclodextrin; Porphyrin; Hemoprotein; Self-assembly

1. Introduction

Nature orchestrates molecular self-assembly on a grand scale through the manipulation of weak inter- and intramolecular forces. Proteins fold and associate cofactors such as hemes using the hydrophobic effect [1,2], electrostatic forces, hydrogen bonding [3] and ligation of the heme-iron to protein-appended ligands. A variety of synthetic model compounds has been described with the aim to understand structure–function relationships of hemoproteins and to reveal how the protein modulates the iron coordination environment to affect the many roles and subtle complexities of these systems. Axial ligands have been introduced in these synthetic molecules via covalent modification of metalloporphyrin periphery as seen in tailed or bridged model compounds [4–8]. The elementary protein superstructure and the required heme-iron site isolation has been mimicked by covalent attachment of bulky groups around the porphyrin core. New self-assembled hemoprotein model compounds have begun to draw attention [9] only recently with the appearance of peptide-heme constructs [10–15]. With proper design, self-assembly offers a simpler and ultimately more flexible approach to novel constructs over tradi-

*Corresponding author. Tel.: +1-609-258-3593 fax: +1-609-258-0348.

E-mail address: jtgroves@princeton.edu (J.T. Groves).

0301-4622/03/$ - see front matter © 2003 Elsevier Science B.V. All rights reserved.
doi:10.1016/S0301-4622(03)00094-2

tional covalent approaches. Thus, for example, self-assembly has been used to impose enzyme-like specificity in a membrane-bound model of cytochrome P450 and to create a multi-heme, transmembrane, electron transfer construct [16–19]. Here we describe the synthesis and characterization of a hemoprotein model assembly, hemodextrin, a minimalist myoglobin, using the hydrophobic binding intrinsic to the central cavity of a cyclodextrin to facilitate the formation of a metalloporphyrin–cyclodextrin inclusion complex. Although cyclodextrin–porphyrin complexes have been drawing attention as building blocks for supramolecules [20], hemodextrin is the first well-characterized, self-assembled, functional hemoprotein model compound. This spontaneously associating, non-protein construct has been found to bind O_2 and CO in the iron(II) state and to form an unusually stable ferryl state.

2. Experimental

2.1. Materials and methods

Fe(III)TPPS [iron(III) *meso*-tetrakis(4-sulphonatophenyl)porphyrin] was purchased from Mid-Century Chemical. Deuterated solvents, anhydrous dimethylsulphoxide (DMSO), sodium hydroxide, β-cyclodextrin, 3-(bromomethyl)pyridine hydrobromide (BMPHBr), tri(ethyleneglycol)monomethyl ether and H_2TCPP [*meso*-tetrakis-(4-carboxyphenyl)porphyrin] were purchased from Aldrich and used without further purification. Molecuar sieve (3 Å) was obtained from EM Science and activated before use. Water was purified by a Milli-Q (Millipore) system. β-cyclodextrin was dried at 100 °C over phosphorous pentoxide under vacuum for 3 days before use.

Nuclear magnetic resonance spectra were collected on a Varian INOVA 500 NMR spectrometer. UV–Vis spectra were obtained on Varian Cary 300 Bio UV–Vis spectrophotometer. Kinetic data was collected on a Hi-Tech SF-61 DX2 rapid-mixing stopped-flow spectrophotometer and analyzed on KinetAssyst software provided by Hi-Tech. The generation and decay of ferryl species was monitored at 421 nm.

2.2. Preparation of ^{1}H-NMR samples

In the binding stoichiometry study, H_2TCPP (1 mg) and excess PPCD (per-PEGylated β-cyclodextrin) (**4**) (23 mg) were added to 1 ml DMSO-d_6. After taking ^{1}H-NMR spectra in DMSO-d_6, 0.1 ml of the above solution was added to 0.9 ml D_2O and ^{1}H-NMR in D_2O was taken.

In the axial ligation study, Fe(III)TPPS (1 mg) and py-PPCD (**2**) (19 mg) were dissolved in D_2O 0.75 ml and the solution was deaerated by 3 freeze-pump-thaw cycles. A 20-fold excess of solid sodium dithionite was added under nitrogen atmosphere. The reduced Fe(II)-3 complex solution was transferred into NMR tube and sealed under nitrogen.

2.3. Dioxygen binding

A round bottom flask and a vacuum adaptor was integrated into a UV cuvette with a light path of 0.1 cm. Fe(III)TPPS (50 μM) and py-PPCD (**2**) (170 μM) in 250 μl pH 6.0 50 mM phosphate buffer in the integrated round bottom flask was strictly deaerated by freeze-pump-thaw: six cycles on a high-vaccum ($<10^{-6}$ mmHg) Schlenk line. The integrated cuvette-flask system was filled with nitrogen and the solution was transferred to the cuvette by inverting the flask. A two-flask chamber with a vacuum adaptor was used to prepare the sodium dithionite solution. Sodium dithionite powder was deposited in one of the flasks and water was transferred to the other flask. Water was deaerated by *f-p-t* and then mixed with solid sodium dithionite by inverting the flasks. To reduce the Fe(III)-**3** to Fe(II)-**3**, a near stoichiometric amount of sodium dithionite solution was added by gas-tight syringe to the UV cuvette. Then, the UV-cuvette was flushed with pure oxygen to form the (O_2)–Fe(II)-**3**. Subsequently, CO gas was introduced to convert the (O_2)–Fe(II)-**3** to (CO)–Fe(II)-**3**.

2.4. Preparation and characterization of the cyclodextrin derivatives

2.4.1. py-CD (*1*) (*2^A-monopyridylmethyl-β-cyclodextrin*)

Dried β-cyclodextrin (2 g) was dissolved in 200 ml of anhydrous DMSO under an argon

atmosphere. Freshly powdered NaOH (0.64 g) was added and then heated at 100 °C for 2 h. 3-(Bromomethyl)pyridine hydrobromide (BMPHBr) (0.4 g) was added at 25 °C and stirred for 3 days. DMSO was distilled away under vacuum and the residue was washed with acetone to give a yellow solid. It was purified on a bonded C18 reversed phase silica gel (Analtech) column eluting with 10–30% methanol in water. The volume of the eluted fractions was reduced and then underwent freeze-dry to give 800 mg of (**1**) as a pale powder. δ_H (500 MHz; DMSO-d_6 and D_2O) 3.35–3.50 (14H, *m*, H_2 and H_4, *d* at 3.5: $H_{2'}$), 3.60–3.65 (7H, *m*, H_5), 3.65–3.75 (20H, *m*, H_6 and H_3 except $H_{3'}$), 3.89 (1H, *t*, $H_{3'}$), 4.81 (2H, *t*, H_7), 4.87–4.94 (6H, *m*, H_1 except $H_{1'}$), 5.03 (1H, *d*, $H_{1'}$), 7.48 (1H, *dd*, H_{10}), 7.90 (1H, *d*, H_9), 8.49 (1H, *d*, H_{11}), 8.55 (1H, *s*, H_{12}); δ_c (500 MHz; DMSO-d_6 and D_2O) 60.13 (C_6), 71.08 (C_7), 72.05 ($C_{3'}$), 72.30 (C_5), 72.47 (C_2), 73.14 (C_3 except $C_{3'}$), 80.36 ($C_{2'}$), 81.71 (C_4 except $C_{4'}$), 82.42 ($C_{4'}$), 100.37 ($C_{1'}$), 102.22 (C_1 except $C_{1'}$), 124.01 (C_{10}), 133.70 (C_8), 136.41 (C_9), 149.31 (C_{11}), 149.42 (C_{12}). HR (FAB) MS ($M+H^+$, $C_{48}H_{76}O_{35}N^+$): calc. mass 1226.41968, exact mass 1226.42400.

2.4.2. py-PPCD (***2***) (*2^A-monopyridylmethyl-per-PEGylated-β-cyclodextrin*)

py-CD (**1**) was dried at 100 °C over P_2O_5 under vacuum for 3 days before use. A 140 mg sample of (**1**) was dissolved in anhydrous DMSO 20 ml under nitrogen atmosphere. Anhydrous benzene 10 ml was added and stirred for 5 min. Molecular sieve 3 Å (1.5 g) was added and stirred for 15 min. The solution was transferred to a clean dry flask and freshly powdered NaOH 188 mg was added. PEG-OTs [tri(ethylene glycol)monomethy ether tosylate] [prepared by reacting tri(ethylene glycol)monomethyl ether with tosyl chloride in CH_2Cl_2 in the presence of triethylamine] 1.2 ml was then added and stirred for 4 days. The reaction solution was poured into 200 ml water, extracted with chloroform. The chloroform layer was washed with saturated aqueous NaCl, dried over anhydrous sodium sulphate and dried under vacuum. The product was purified on a silica gel column eluting with 1–4% methanol in chloroform to afford 98 mg of (2), obtained as a colorless oil; δ_H (500 MHz; $CDCl_3$) 3.34–3.40 (60H, *m*, OCH_3), 3.58–3.68 (240H, *m*, CH_2 on PEG-3 tails), 3.2–4.2 (42H, *m*, H on cyclodextrin skeleton), 4.76–4.92 (2H, *q*, py-CH_2), 5.15-5.27 (7H, *m*, anomeric H on cyclodextrin), 7.30 (1H, *dd*, py-H_4), 7.85 (1H, *d*, py-H_3), 8.52 (1H, *d*, py-H_5), 8.61 (1H, *s*, py-H_1); δ_c (500 MHz; $CDCl_3$) 59.00, 69.69, 70.25–70.59, 70.97, 71.06, 71.28, 71.94, 72.72, 73.04,77.60–79.11, 80.55–81.12, 98.02, 98.16, 123.38 (py-C_4), 134.55 (py-C_2), 135.85 (py-C_3), 148.84 (py-C_5), 149.20 (py-C_1). MS (MALDI-TOF): m/z 4145.6. Chem. Anal. Calcd: C, 53.26; H, 8.68; N, 0.33; Found: C, 53.16; H, 8.73; N, 0.32.

3. Results and discussion

It has been reported that heptakis(2,3,6-tri-*O*-methyl)-β-cyclodextrin (TMCD) and *meso*-tetraphenyl porphyrins formed 2:1 complexes with a significantly high affinity [21]. Two TMCD molecules are *trans* to one. NOE experiments showed the secondary side of TMCD faced toward the center of the porphyrin with the *meso*-aryl group of the porphyrin occupying the cyclodextrin core. A 1:1 binding mode and a properly positioned axial ligand were desired in our approach (Fig. 1) to construct an artificial heme-binding pocket. Based on molecular modeling studies using Chem3D, py-PPCD (**2**) (monopyridyl-per-PEGylated β-cyclodextrin) (Fig. 2) was designed as the target molecule. Upon binding to one of the pendant aryl groups of a *meso*-tetraphenyl porphyrin, the PEG tails of py-PPCD (**2**) were anticipated to span the entire porphyrin plane and block the second CD binding site. Furthermore, the PEG appendages were considered to be flexible enough to allow access to the metal center by reactants, and would serve to keep the cyclodextrin–porphyrin molecule soluble in water. Water solubility would allow us to perform biologically relevant reactions with control over pH and ionic strength. Furthermore, our modeling studies showed that the pyridyl nitrogen attached to the 2′-OH of CD was positioned to allow coordination to the metal center of all associated porphyrins.

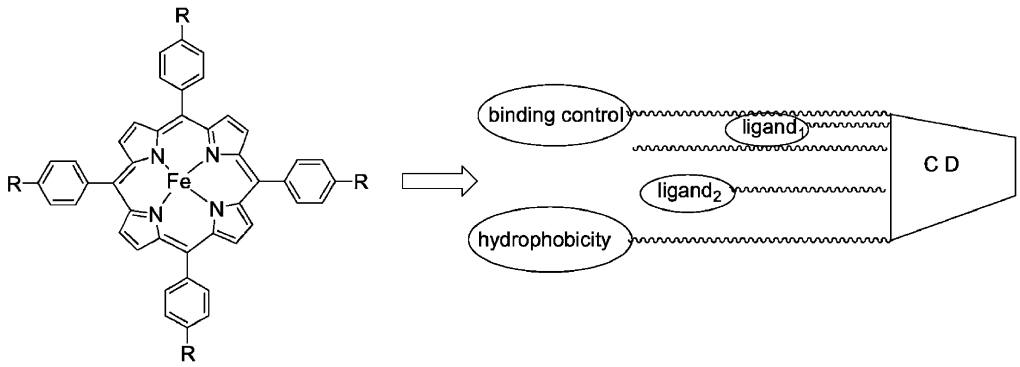

Fig. 1. Design of self-assembled hemodextrin inclusion complexes.

In order to prove that the PEG tails were sufficient to block the second binding site on tetraphenyl porphyrins, PPCD [perPEGylated-β-cyclodextrin] (**bb**) was synthesized by peralkylation of β-cyclodextrin with tri(ethylene glycol) monomethyl ether tosylate (PEG-OTs) and its binding with *meso*-tetraphenyl porphyrins was investigated. The 1:1 stoichiometry of the porphyrin and PPCD binding was determined from the ^{1}H-NMR of the complex of PPCD and H_2TCPP [*meso*-tetra(4-carboxyphenyl)porphyrin] in D_2O. The 16 *ortho*- and *meta*-phenyl protons of the *para*-substituted porphyrin representing eight AB systems would give only two doublets with integrals in the ratio of 8:8 with no binding of the cyclodextrin, 4 doublets in the ratio of 4:4:4:4

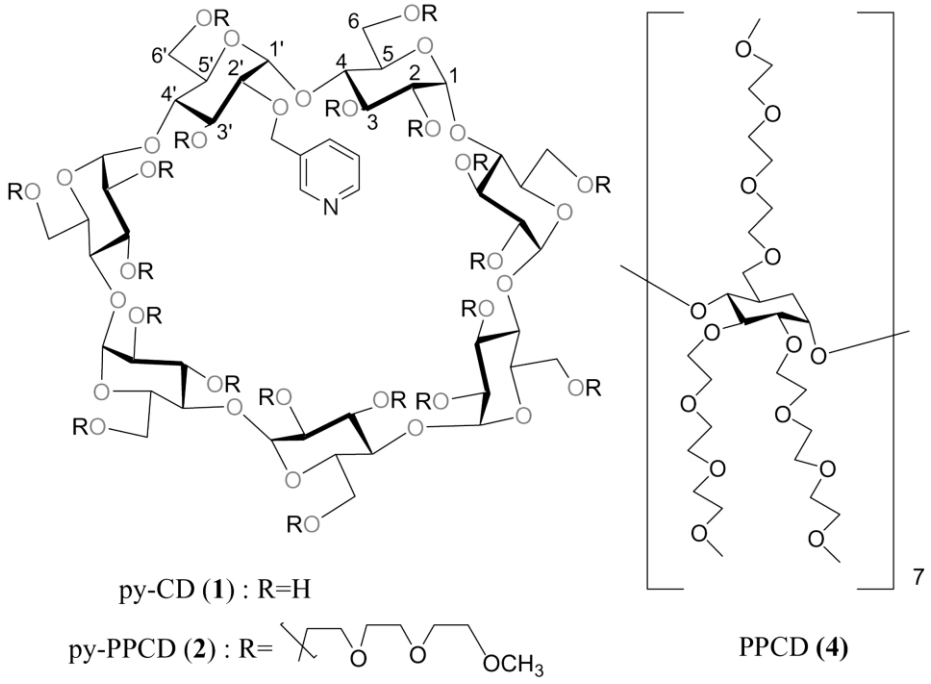

Fig. 2. Structures of py-CD (**1**), py-PPCD (**2**) and PPCD (**4**).

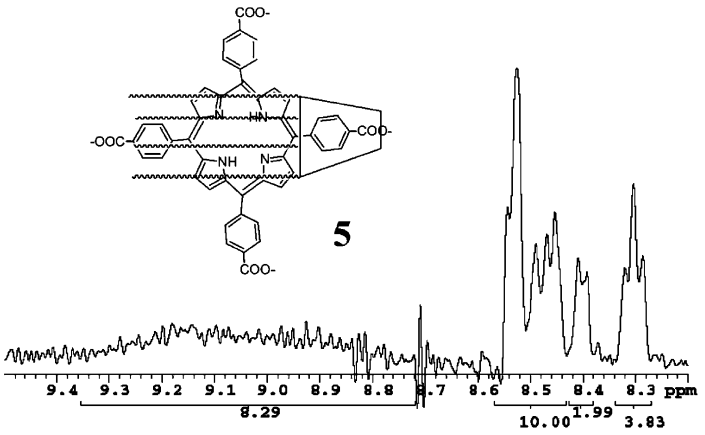

Fig. 3. ^{1}H-NMR of (H_2TCPP + PPCD) (**5**) in D_2O (90%) and DMSO-*d*6 (10%). The *meso*-aryl and β-pyrrole protons of H_2TCPP are shown.

with a 1:2 porphyrin–cyclodextrin binding mode, and 6 doublets in the ratio of 2:2:2:2:4:4 with a 1:1 binding mode. The phenyl protons in the NMR spectrum of (PPCD + H_2TCPP) (**5**) (Fig. 3) complex were observed to be split into a doublet, a triplet and a multiplet in the ratio of 2:4:10, which was consistent only with a 1:1 binding stoichiometry(Fig. 3). Interestingly, (PPCD + H_2TCPP) in DMSO-d_6 gave two doublets in the ratio of 8:8 for the phenyl protons mentioned above. This indicated no binding in DMSO, which might be due to the blockage of the sugar cavity by self-aggregated PEG chains. In water, formation of hydrogen bonds could be a good driving force for the PEG's to become solvated instead of aggregating, thus made the binding cavity accessible.

The modified cyclodextrin construct Py-CD (**1**) (Fig. 2), with a pyridyl group appended to one of the 2′-hydroxy groups of the heptamylose sugars of β-cyclodextrin, was successfully prepared in 30% yield by treatment of β-cyclodextrin with 3-(bromomethyl)pyridine hydrobromide (BMPHBr) and powdered NaOH in dry DMSO [22] followed by a C18 reversed phase column. The product was clearly mono-substituted as shown by the HRMS (FAB) mass signal at 1226.42400 (calculated mass 1226.41968) and the ^{1}H-NMR, showing four pyridyl protons at δ 7.5–8.6, seven anomeric protons at δ 4.9–5.0 and two diastereotopic H-7 protons as a triplet at δ 4.8. The 8 ppm downfield shift of C-2′ and 2 ppm upfield shift of C-1′ in the ^{13}C-NMR of **1**, away from those of CD unmodified C-2 and C-1 clearly indicated the substitution was at 2′-position [23]. It is interesting to note that the water-soluble β-cyclodextrin became insoluble after attachment of the pyridyl group. Upon addition of *p*-iodophenol, which is a good guest for the sugar cavity, py-CD (**1**) became water-soluble. NOE experiments on py-CD (**1**) in DMSO-d_6 showed correlation signals between the pyridyl proton H-9 and β-cyclodextrin protons H-3,5 which were located inside the cavity. This indicated that the pyridyl was included inside the cavity. The above observations indicated the formation of a 'non-covalent polymer' (Fig. 4) as has been observed by Hoshino and Harata et al. [24] through intermolecular inclusion.

Treatment of Py-CD (**1**) with tri(ethylene glycol) monomethyl ether tosylate (PEG-OTs) and freshly powdered NaOH in dry DMSO provided a mixture of alkylated products with 8–20 PEG groups as shown by the evenly spaced MALDI-TOF mass spectroscopy signals. Past attempts to attach long alkyl chains to cyclodextrins have been reported to give an inseparable mixture of products with an average of 18 alkyl chains [25]. The inefficient alkylation of **1** was due to the formation of the non-covalent polymer, which buried the hydroxyls thus, made them difficult to be attacked by the alkylating reagent (Fig. 4). Addition of

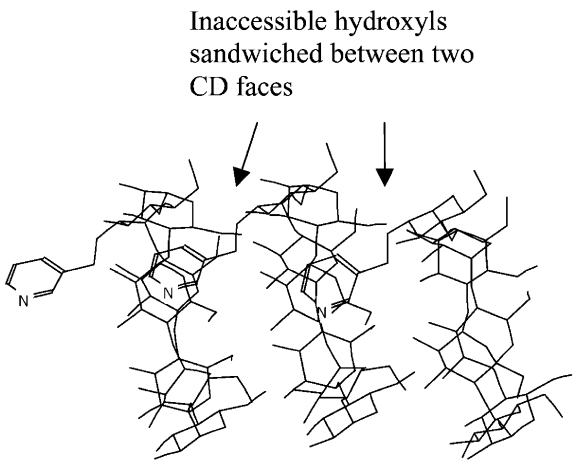

Fig. 4. Likely structure of the insoluble inclusion non-covalent polymer of (**1**).

guest molecules such as benzene served to dissociate the polymer and facilitate the alkylation. Indeed, upon addition of benzene to the above reaction, monopyridyl-perPEGylated β-cyclodextrin py-PPCD (**2**) was obtained in 21% yield as a fully alkylated single product as evidenced by a single m/z at 4145 in MALDI-TOF mass spectroscopy and elemental analysis as shown in the experimental section.

meso-Tetra(4-sulphonatophenyl)porphyrin [Fe(III)TPPS] was used as the porphyrin core in the following studies because it is easy to purify and has satisfactory solubility at a wide range of pH's. The binding affinity between Py-PPCD (**2**) and iron(III) *meso*-tetra(4-sulphonatophenyl)porphyrin [Fe(III)TPPS] was measured by UV–Vis titration at pH 6.0. Upon binding, the Soret of the porphyrin shifted from 394 to 402 nm with a decrease in intensity. Absorption at 394 nm was monitored and fitted into a single site binding equation using Scientist™ software to give a binding constant of 2.4×10^6 M^{-1} at pH 6.0. A series of amphiphilic two-α-helix peptides has been reported to bind heme with binding constants ranging 10^6–10^7 M^{-1} [26]. The cyclodextrin–porphyrin binding constant of **2** thus is comparable to the known peptide-heme binding constants. The py-PPCD (**2**) proved to be a robust single site metalloporphyrin binding pocket even at micromolar concentrations.

Porphyrin binding and ligation of the pyridyl nitrogen to the iron in **2** was confirmed by the ^{1}H-NMR of the complex (**3**) between Py-PPCD (**2**) and Fe(II)TPPS. The chemical shift of the β-pyrrole protons served as a good indicator for the coordination environment of Fe(II)porphyrins. Four-coordinate square planar intermediate spin Fe(II) porphyrins have their β-pyrrole protons in the diamagnetic region, while for five-coordinate high spin Fe(II) porphyrins the resonances appear in the downfield region of ~δ 40–60 [27]. Fe(II)TPPS showed all of its protons in the diamagnetic region of δ 0–9, but the pyrrole protons shifted to the region of δ 40–60 upon addition of py-PPCD (**2**) or upon addition of TMCD (permethylated β-cyclodextrin) and 2-methyl imidazole [28] as a standard five-coordinate high spin model (Fig. 5). This unambiguously established the five-coordinate, high spin iron(II) center in the

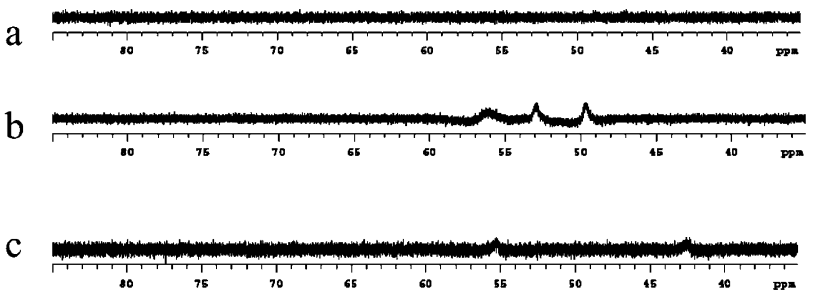

Fig. 5. ^{1}H-NMR of (H_2TCPP + PPCD) (a) Fe(II) TPPS; (b) Fe(II)TPPS and py-PPCD [complex Fe(II)-**3**]; (c) Fe(II)TPPS, TMCD and 2-methyl imidazole in D_2O.

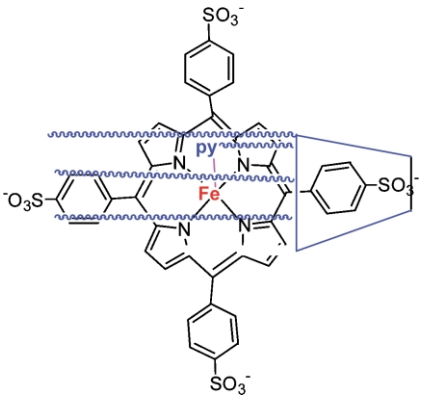

Fig. 6. Illustration of (FeTPPS + py-PPCD): complex (**3**).

self-assembled hemoprotein model compound (**2**) (Fig. 6).

Ferric hemoproteins such as met-myoglobin are known to have water as the sixth ligand to its ferric center at low pH, while they have hydroxide ion as the sixth ligand at high pH [29]. Our water soluble hemoprotein model compound (**3**) in its ferric form showed a Soret shift from 402 nm at pH 6.0–418 nm at pH 7.4, suggesting a deprotonation process at this pH range. When the pH was raised to 10.4, the porphyrin dimerized with a Soret at 410 nm. In the absence of py-PPCD (**2**), Fe(III)TPPS dimerized above pH 6 with a Soret shift from 394 to 410 nm. It is clear that the metalloporphyrin binding pocket py-PPCD (**2**) effectively inhibited the dimerization process.

The ability of hemoproteins to bind small gaseous ligands is central to their functions [30,31]. The oxygen binding properties of many different hemoprotein model compounds have been extensively studied in the past three decades [7]. It is noteworthy that all of the model compounds studied before were constructed via covalent attachment of bulky groups and axial ligands in order to inhibit the porphyrin dimerization and stabilize the oxygen adducts. Thus, it is of interest that hemodextrin [Fe(II)-**3**] bound the O_2 and CO. The ferric complex **3** was reduced to the ferrous form in deaerated pH 6.0 aqueous phosphate buffer by the near-stoichiometric addition of sodium dithionite [32]. The Soret absorbance of the ferric complex Fe(III)-**3** shifted from 402 to 437 nm as it was converted to ferrous form Fe(II)-**3**. After opening the system to air, the absorption at 437 nm decreased while a broad peak at 417 nm appeared signaling the formation of a new intermediate. Exposure of this intermediate to CO afforded immediately a ferrous-CO adduct (CO)–Fe(II)-**3** with a Soret absorbance at 422 nm. This transformation allowed the assignment of the 417 nm intermediate as the ferrous-O_2 adduct (O_2)–Fe(II)-**3** (Fig. 7). The visible spectrum of the reaction mixture containing the CO adduct also showed a shoulder at 402 nm indicating partial autoxidation to the ferric form Fe(III)-**3**. This behavior is similar to the oxygenated forms of myoglobin and hemoglobin that oxidize spontaneously to the ferric (met) form [33]. The oxy form of hemodextrin, (O_2)–Fe(II)-**3**, was remarkably stable, decomposing to the ferric form in the course of several hours. The ferrous-CO adduct of **3** was stable for at least 2 days. The stabilities of the (O_2)–Fe(II)-**3** and (CO)–Fe(II)-**3** forms of our self-assembled model compound compare favorably with the most

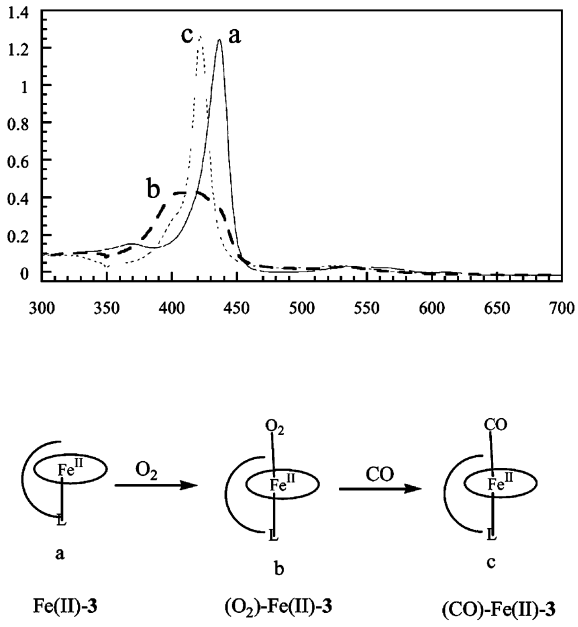

Fig. 7. UV–Vis spectra of complex (**3**) in reduced Fe(II) form (solid line a); its oxygenated form (O_2)–Fe(II)-**3** converted from (O_2)–Fe(II)-**3** (dotted line c) 50 μM in pH 6.0 50 nM phosphate buffer.

Table 1
Reaction of FeTPPS with excess peroxynitrite in 100 nM pH 7.4 phosphate buffer, k_1 is oxidation of Fe(III) to Fe(IV), k_2 is Fe(IV) decay back to Fe(III)

Metalloporphyrins	k_1 ($M^{-1}s^{-1}$)	k_2 (s^{-1})
FeTPPS + py-PPCD	1.4×10^5	0.11
FeTPPS	2.0×10^4	1.65

recent dentritic model [8] that binds dioxygen at room temperature.

The ferryl state of hemoproteins is associated with important oxidation and electron transfer reactions in biological system [30,31]. We have found that the ferryl state of the (FeTPPS + py-PPCD) complex **3** was unusually stable as well. Reaction of Fe(III)-**3** with excess peroxynitrite gave a new species with a stronger Soret at 421 nm. This new species was assigned to the oxoFe(IV) form based on comparisons to a number of oxoFe(IV) porphyrins we have reported recently [34–36]. As we have observed in the past, Fe(III) porphyrins are converted to Fe(IV) porphyrins with a red shift and intensity increase of Soret band and the unstable Fe(IV) form decays back to Fe(III) form. Stopped-flow experiments in 100 mM pH 7.4 phosphate buffer showed that upon oxidation by peroxynitrite [oxoFe(IV)TPPS + py-PPCD] was formed at a rate of 1.4×10^5 $M^{-1}s^{-1}$ which is 7 times faster than oxoFe(IV)TPPS. The [oxoFe(IV)TPPS + py-PPCD] was 15 times more stable with respect to spontaneous reduction to the resting Fe(III) state than oxoFe(IV)TPPS. The above rate constants are shown in Table 1. Accordingly, we conclude that the pyridyl ligation has accelerated the production of ferryl and stabilized the ferryl species due to the electron donating ('push') effect of the pyridyl ligand which facilitated the cleavage of O–O bond and stabilized the high valent electron deficient ferryl species [37,38].

4. Summary and conclusion

The synthesis and characterization of the self-assembled hemoprotein model hemodextrin (**3**) (Fig. 8) described here can be extended to a general strategy for the synthesis of a series of

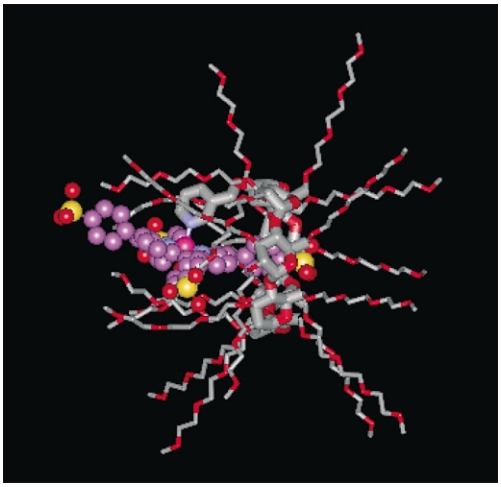

Fig. 8. 3-D molecular model of the Hemodextrin (**3**): complex between py-PPCD and Fe(III)TPPS. Chem3D was used to minimize energy and weblab Viewlite was used for graphics. The carbon skeleton of Fe(III)TPPS is in purple for clarity. Nitrogen: blue; Oxygen: red; Carbon: grey; Sulphur: yellow; Iron: pink.

self-assembled hemoprotein model compounds with different functionalities in the region of the heme group. The rim of the cyclodextrin bucket is designed to be the 'handle' to attach desired functional groups in order to control stoichiometry, introduce proximal or distal ligands, control hydrophobicity, etc. A suitably designed cyclodextrin has the potential to serve as an artificial apohemoprotein to incorporate metalloporphyrins and fulfill a variety of functions [39].

Acknowledgments

This paper is dedicated to our dear colleague Walter Kauzmann who inspired these studies through his conceptualization of the hydrophobic effect. Support by the National Science Foundation and the National Institutes of Health (GM36928) is gratefully acknowledged. HRMS was provided by the Washington University Mass Spectrometry Resource with support from the NIH National Center for Research Resources (Grant No. P41RR0954). We thank Dr Carlos Pacheco and Dr Istvan Pelczer for assistance in btaining NMR and Dr Dorothy Little for obtaining mass spectra.

We thank Dr Tommaso Carofiglio, University of Padua, for his valuable suggestions and discussions.

References

[1] W. Kauzmann, Some factors in the interpretation of protein denaturation, Adv. Protein Chem. 14 (1959) 1–63.
[2] W. Kauzmann, Protein stabilization—Thermodynamics of unfolding, Nature 325 (1987) 763–764.
[3] K.H. Choi, A.D. Hamilton, Selective anion binding by a macrocycle with convergent hydrogen bonding functionality, J. Am. Chem. Soc. 123 (2001) 2456–2457.
[4] J.P. Collman, Functional analogs of heme protein active sites, Inorg. Chem. 36 (1997) 5145–5155.
[5] H. Volz, M. Holzbecher, A bridged porphyrinato(thiolato)iron(III) complex as a model of the active center of the cytochrome P-450 isozyme, Angew. Chem. Int. Edit. Engl. 36 (1997) 1442–1445.
[6] R. Breslow, X.J. Zhang, Y. Huang, Selective catalytic hydroxylation of a steroid by an artificial cytochrome P-450 enzyme, J. Am. Chem. Soc. 119 (1997) 4535–4536.
[7] M. Momenteau, C.A. Reed, Synthetic heme dioxygen complexes, Chem. Rev. 94 (1994) 659–698.
[8] P. Weyermann, F. Diederich, Synthesis of dendritic iron(II) porphyrins with a tethered axial imidazole ligand designed as new model compounds for globins, J. Chem. Soc. Perkin Trans. 1 (2000) 4231–4233.
[9] T. Komatsu, S. Hayakawa, T. Yanagimoto, M. Kobayakawa, A. Nakagawa, E. Tsuchida, Iron(II) complex of octopus-porphyrin with a covalently linked proximal imidazole; self-assembly and *O*-2-coordination in aqueous media, B. Chem. Soc. Jpn. 74 (2001) 1703–1707.
[10] D.A. Moffet, L.K. Certain, A.J. Smith, A.J. Kessel, K.A. Beckwith, M.H. Hecht, Peroxidase activity in heme proteins derived from a designed combinatorial library, J. Am. Chem. Soc. 122 (2000) 7612–7613.
[11] D.L. Huffman, M.M. Rosenblatt, K.S. Suslick, Synthetic heme-peptide complexes, J. Am. Chem. Soc. 120 (1998) 6183–6184.
[12] P.A. Arnold, W.R. Shelton, D.R. Benson, Peptide helix induction in a self-assembling hemoprotein model, J. Am. Chem. Soc. 119 (1997) 3181–3182.
[13] C.M. Summa, M.M. Rosenblatt, J.K. Hong, J.D. Lear, W.F. Degrado, Computational de novo design, and characterization of an A(2)B(2) diiron protein, J. Mol. Biol. 321 (2002) 923–938.
[14] F. Rabanal, W.F. Degrado, P.L. Dutton, Toward the synthesis of a photosynthetic reaction center maquette: A cofacial porphyrin pair assembled between two subunits of a synthetic four-helix bundle multiheme protein, J. Am. Chem. Soc. 118 (1996) 473–474.
[15] K.S. Akerfeldt, R.M. Kim, D. Camac, J.T. Groves, J.D. Lear, W.F. Degrado, Tetraphilin- a 4-helix proton channel built on a tetraphenylporphyrin framework, J. Am. Chem. Soc. 114 (1992) 9656–9657.
[16] G.F. Xu, N. Yao, I.A. Aksay, J.T. Groves, Biomimetic synthesis of macroscopic-scale calcium carbonate thin films. Evidence for a multistep assembly process, J. Am. Chem. Soc. 120 (1998) 11977–11985.
[17] J.T. Groves, Artificial enzymes—The importance of being selective, Nature 389 (1997) 329–330.
[18] J. Lahiri, G.D. Fate, S.B. Ungashe, J.T. Groves, Multiheme self-assembly in phopholipic vesicles, J. Am. Chem. Soc. 118 (1996) 2347–2358.
[19] J.T. Groves, R. Neumann, Regioselective oxidation catalysis in synthetic phospholipid-vesicles-membrane-spanning steroidal metalloporphyrins, J. Am. Chem. Soc. 111 (1989) 2900–2909.
[20] T. Jiang, D.S. Lawrence, Sugar-coated metalated macrocycles, J. Am. Chem. Soc. 117 (1995) 1857–1858.
[21] T. Carofiglio, R. Fornasier, V. Lucchini, C. Rosso, U. Tonellato, Very strong binding and mode of complexation of water-soluble porphyrins with a permethylated beta-cyclodextrin, Tetrahedron Lett. 37 (1996) 8019–8022.
[22] Y. Ishimaru, T. Masuda, T. Iida, Synthesis of secondary face-to-face cyclodextrin dimers linked at each 2-position, Tetrahedron Lett. 38 (1997) 3743–3744.
[23] A. Ueno, R. Breslow, Selective sulphonation of a secondary hydroxyl group of beta-cyclodextrin, Tetrahedron Lett. 23 (1982) 3451–3454.
[24] T. Hoshino, M. Miyauchi, Y. Kawaguchi, H. Yamaguchi, A. Harada, Daisy chain necklace: Tri 2 rotaxane containing cyclodextrins, J. Am. Chem. Soc. 122 (2000) 9876–9877.
[25] P.S. Bates, R. Kataky, D. Parker, Selective binding and detection of onium ions by lipophilic neutral cyclodextrins, J. Chem. Soc. Chem. Commun. (1993) 691–693.
[26] S. Sakamoto, I. Obataya, A. Ueno, H. Mihara, Effects of amino acids substitution of hydrophobic residues on haem-binding properties of designed two-alpha-helix peptides, J. Chem. Soc. Perkin Trans. 2 (1999) 2059–2069.
[27] F.A. Walker, Proton NMR and EPR spectroscopy of paramagnetic metalloporphyrins, in: K.M. Kadish, K.M. Smith, R. Guilard (Eds.), The Porphyrin Handbook, Academic Press, San Diego, CA, 2000, pp. 81–175.
[28] J.P. Collman, C.A. Reed, Syntheses of ferrous-porphyrin complexes-hypothetical model for deoxymyoglobin, J. Am. Chem. Soc. 95 (1973) 2048–2049.
[29] T. Yoshida, C.T. Migita, Mechanism of heme degradation by heme oxygenase, J. Inorg. Biochem. 82 (2000) 33–41.
[30] J.T. Groves, K. Shalyaev, J. Lee, Oxometalloporphyrins in Oxidative Catalysis, in: K.M. Kadish, K.M. Smith, R. Guilard (Eds.), The Porphyrin Handbook, Academic Press, San Diego, 2000, pp. 17–40.

[31] J.T. Groves, Y.Z. Han, Models and mechanisms of cytochrome P-450 action, in: P.R. Ortiz de Montellano (Ed.), Cytochrome P-450 Structure, Mechanism and Biochemistry, Plenum Press, New York, 1995, pp. 1–45.
[32] A.A. Elawady, P.C. Wilkins, R.G. Wilkins, Kinetic aspects of the iron(III)-Tetrakis(*para*-sulphonatophenyl)porphine system, Inorg. Chem. 24 (1985) 2053–2057.
[33] K. Shikama, The molecular mechanism of autoxidation for myoglobin and hemoglobin: A venerable puzzle, Chem. Rev. 98 (1998) 1357–1373.
[34] J.B. Lee, J.A. Hunt, J.T. Groves, Mechanisms of iron porphyrin reactions with peroxynitrite, J. Am. Chem. Soc. 120 (1998) 7493–7501.
[35] R. Shimanovich, J.T. Groves, Mechanisms of peroxynitrite decomposition catalyzed by FeTMPS, a bioactive sulphonated iron porphyrin, Arch. Biochem. Biophys. 387 (2001) 307–317.
[36] J.L. Bourassa, E.P. Ives, A.L. Marqueling, R. Shimanovich, J.T. Groves, Myoglobin catalyzes its own nitration, J. Am. Chem. Soc. 123 (2001) 5142–5143.
[37] J.H. Dawson, Probing structure-function relations in heme-containing oxygenases and peroxidases, Science 240 (1988) 433–439.
[38] T.L. Poulos, The role of the proximal ligand in heme enzymes, J. Biol. Inorg. Chem. 1 (1996) 356–359.
[39] T. Komatsu, S. Hayakawa, E. Tsuchida, H. Nishide, *meso*-Tetrakis[O-(N-methyl)pyridinium] porphyrin ensembles with axially coordinated cyclodextrin-penetrating phenethylimidazole: reversible dioxygen binding is aqueous DMF solution, Chem. Commun. 2003, 60–61.